Chapter 2

Literature Review

CHAPTER-2
Literature Review

ZnO has the potential to be a highly multifunctional material with coexisting semiconducting, electromechanical, magnetic, and optical properties. Despite of it being great promise as a device material, limited success has been achieved till date. This lack of rapid progress is due, in part, to a lack of understanding of the role of various defects in ZnO material and their effect on device performance. ZnO, with different morphologies and less native defects, is found to be important functional material to accommodate a large variety of applications. Control of the morphology of ZnO is essentially required to fulfill the production of future generation of smart and functional materials. The novel properties of nanomaterials depend on their size and shape as the various facets or directions in a crystal may exhibit different physical as well as chemical properties. Therefore, new synthetic strategies and a better understanding of the growth mechanisms are necessary. In this chapter, the synthesis techniques developed for ZnO are discussed in Section 2.1. In Section 2.2, the role of native defects in ZnO which is typically responsible for n-type conduction, magnetic ordering and the defect induced luminescence transitions in ZnO are explained. Section 2.3 involves the studies of doping and codoping in ZnO and their affect on optical as well as magnetic properties. Section 2.4 deals with the studies on different ceramic composites, in particular ZnO based ceramic composites. We present the objective of the present work in Section 2.5.

2.1 Synthesis of ZnO

Recent research has demonstrated the formation of ZnO in highly oriented and ordered arrays. ZnO nanostructures, such as nanodots [Xu *et al.* (2005)], nanowires (NWs) [Huang *et al.* (2001)], nanorods (NRs) [Guo *et al.* (2002)], nanobelts [Pan *et al.* (2001)], nanorings [Kong *et al.* (2004)], nanotubes (NTs) [Zhang *et al.* (2002)], nanocages [Fan *et al.* (2004)] and hierarchical patterns, etc. [Lao *et al.* (2002)] have been prepared by different

methods. These structures have been synthesised under controlled growth conditions. There have been many existing preparative techniques for ZnO. In literature, we found various reports of the high-temperature growth techniques such as metal-organic chemical vapor deposition (MOCVD) [Kim *et al.* (2003)], vapour phase transport (VPT), [Ng *et al.* (2003)] vapour-liquid-solid epitaxial (VLSE) mechanisms, [Yang *et al.* (2012); Lyu *et al.* (2002); Gao *et al.* (2004); Zhang *et al.* (2003)] vapour-phase epitaxy, [Roy *et al.* (2003)] template-assisted growth [Jiansheng *et al.* (2004)]. These gas-phase approaches generally require high temperature and expensive equipments. The main limitation of these epitaxial growth methods is that the crystals are attached to a substrate or embedded in a matrix. Most of the substrates are insulating, relatively expensive and not compatible with semiconductor integrated techniques, which limits the range of possible applications of ZnO nanostructures in photonic and electronic devices. On the other hand, some low-temperature growth techniques such as chemical reactions from aqueous solutions,[Vayssieres *et al.* (2003)] and electrochemical techniques [Li *et al.* (2000); Zheng *et al.* (2002)] have been used successfully for the synthesis of highly oriented arrays of anisotropic ZnO with different shapes. Few well known chemical reactions for ZnO synthesis are microemulsion, sol-gel, solvothermal, hydrothermal, combustion and precipitation. Some of the techniques are discussed below.

2.1.1 Hydrothermal Technique

Hydrothermal synthesis is a method that utilizes single or heterogeneous phase reactions in aqueous media at elevated temperature ($T > 25°C$) and pressure ($P > 100$ kPa) to crystallize ceramic materials directly from the solution. For the synthesis of ZnO nanostructures or single crystsls, unlike to high temperature gas-phase approaches, hydrothermal process is one of the most energy-efficient methods that do not have any need of high temperature and complex vacuum environment. In hydrothermal process, easily different morphologies of ZnO can be produced through slight changes in the reaction conditions like temperature, pressure, solvent, gas environments, pH etc.

[Sugunan *et al.* (2006)]. Using hydrothermal synthesis technique, Nishizawa *et al.* (1984) have synthesised needle-like ZnO crystals by decomposition of aqueous solution of Na_2Zn-EDTA at 330 ^{o}C. Lu *et al.* (2000) have produced ZnO after dehydration of $Zn(OH)_2$ in a hydrothermal setup maintained at temperature above to 100 ^{o}C. Recently, by using cetyltrimethylammonium bromide (CTAB) and keeping chemical reaction at 180 ^{o}C for 24 h, ZnO nanorods have been synthesised by Sun *et al*. (2003). Shin *et al*. (2010) have investigated the effects of both *p*H value and presence of a buffer layer on ZnO nanostructure growth on flexible PES substrates. The *p*H value is found to affect the morphology and structural properties of hydrothermally grown ZnO. It is observed that hexagonal shape of ZnO is the most likely shape to occur at *p*H of 7.5, and above *p*H of 8, the morphology changes to an intermediate flower-like morphology [Shin *et al.*, (2010)]. Furthermore, without using any surfactants micron-size ZnO crystals are fabricated through $Zn(OH)_2$ precursor [Jiang *et al*. (2007); Shin *et al*. (2010)]. Several other works on the synthesis of ZnO through hydrothermal method with different morphologies like nanorods, nanowires, nano needles and hierarchical patterns, are reported [Jiang *et al*. (2007)]. The hydrothermal process induces an epitaxial, anisotropic crystal growth in a solution [Hossain *et al.* (2005); Vayssieres *et al.* (2001)]. The substrates like Si [Lee *et al.* (2003)], glass [Sugunan *et al.* (2006); Wei *et al.* (2005)], TCO [Tang *et al.* (2007)], polyethylene fibers [Baruah *et al.* (2008)], carbon cloth [Jo *et al.* (2004)] and Al foil [Umar *et al.* 2007] are frequently used for successful epitaxial growth of ZnO under the hydrothermal process. In this method, syntheses are generally conceded at autogenous pressure, which generates saturated vapour pressure of the solution at a particular temperature and composition of the hydrothermal solution. Normally, mild conditions of temperatures ($\leq$ 350 ^{o}C) and pressures ($\leq$ 50 MPa) are preferred for commercial production of ZnO.

Powder production under hydrothermal process consumes less time and energy because in this process high temperature calcination, mixing, and milling steps are either not necessary or minimized. Uniformity of nucleation,

growth and aging in all over the solution results in improved morphology and size of crystallites and reduced aggregation levels [Riman *et al.* (1993)]. However, water-related lattice defects are among the most common impurities and their concentration determines essential properties of these materials. The problem of water incorporation can be overcome by either properly adjusting the synthesis conditions or by use of non-aqueous solvents (solvothermal processing) [Suchanek *et al.*, (2006)].

2.1.2 Co-precipitation Technique

Controlled precipitation is a extensively used method to synthesise ZnO, since it makes it likely to get a product with repeatable properties. Most of the synthesis techniques utilize different types of substrate (as a seed layer) including the addition of auxiliary agents such as organic ligands and metal-ion impurities to grow various morphologies. In particular, precipitation reactions in unpressurised aqueous media offer relatively low cost, high yield and more controllable process compared to other methods of synthesis and have the potential to scale-up production without any use of surfactant or substrate. In the case of ZnO synthesis, precipitation method involves fast and spontaneous reduction of a solution of zinc salt by using a reducing agent. The most probable zinc salts are zinc nitrate, zinc chloride, zinc sulphate, zinc carbonate and zinc acetate. NaOH, KOH, LiOH and NH_4OH can be used as a reducing agent. The precipitation process is normally initiated by the formation of an amorphous zinc hydroxide, to a crystallized hydroxide after that zinc hydroxide transforms into solid ZnO nuclei by thermal decomposition/dehydration processes. There is still considerable uncertainty regarding the possible role of zinc hydroxide in the mechanism by which the zinc hydroxide (if it forms) converts to zinc oxide, and the factors effecting product morphology. The shape and size of crystals formed from aqueous solutions is quite variable with slight variation in any parameter of the reaction. In a report of Jia *et al.* (2012), the transformation mechanism from $Zn(OH)_2$ to ZnO is demonstrated. Using $ZnCl_2$ and NH_4OH precursors and the cationic surfactant CTAB (cetyltrimethylammonium bromide), Wang *et al.* (2002) have synthesised

highly crystalline ZnO with small and well-dispersed spherical nanoparticles. Various shapes of ZnO like forms resembling rice grains, nuts and rods have been synthesised by Li *et al.* (2005) by using, $Zn(NO_3)_2 \cdot 6H_2O$ and NaOH as precursors and sodium dodecyl sulfate (SDS) and triethanolamine (TEA) as cationic surfactants [Li *et al.* (2005)]. Also, several studies have examined the very significant effects of change in various growth parameters such as stirring, temperature or *p*H on the morphology of the product [Zhang *et al.* (2005), Zhang *et al.* (2005), Govender *et al.* (2004)].

2.1.3 Sol-gel Technique

Sol-gel technique receives considerable attention to produce several morphologies with high purity of ZnO such as films, fibres, and nanostructured materials [Qui *et al.* (2007); Dev *et al.* (2006)]. The sol-gel method possesses low processing temperature, inexpensive, ease of composition control, reliable, repeatable, and simple with good homogeneity. At a time, the powder samples as well as thin film can be manufactured by the Sol-gel technique. Using the sol, spray-drying, fibres spun or drown are the process to produce powder. On the other hand, with the help of spin coating or dip coating techniques thin film can be obtained by using the same sol [Znaidi *et al.* (2010)]. The use of organic precursors like metal acetate and alcoholic solvent are advantageous to be used as an ingredient for sol-gel because the unwanted contaminants decompose under annealing as volatile by-products. Benhebal *et al.* (2013) have prepared spherically shaped ZnO particles by sol-gel method from zinc acetate dihydrate, oxalic acid, using ethanol as solvent. High-filling, unifrom, ordered ZnO nanotubes have been successully prepared by sol-gel method into ultrathin AAO membrane [Yue *et al.* (2013)] The sol-gel method is used to obtain nanocrystalline zinc oxide by using tetramethylammonium hydroxide (TMAH) [Ristić *et al.* (2005)]. TMAH is a strong organic base with the *p*H value of ~14. This high *p*H organic base means that metal oxides are not contaminated with the cation, unlike the case of inorganic base (e.g., NaOH) which may have an effect on the ohmic conductance of the oxide material. Therefore, sol-gel processes avoid the problems presented by certain inorganic anions which

remain in solution during synthesis through co-precipitation, combustion and hydrothermal techniques. However, the large scale production of ZnO powder through sol-gel method is not easy and it consumes time.

2.1.4 Combustion Technique

Solution combustion method generally produces powder "ready to use" with better energy efficiency, with high production rate [Kashinath *et al*. (2002)]. Combustion process is an exothermic reaction in between metal nitrates and fuel at low temperatures, where citric acid ($C_6H_8O_7$) [Roy *et al*. (1999)], carbohydrazide (CH_6N_4O), glycine ($C_2H_5NO_2$) [Mimani *et al.* (2001, 2001(b))] or urea (CH_4N_2O) [Bhaduri *et al*. (1998, 1999); Sousa *et al*. (1999)] etc. can be used as a fuel. The fuel ignition provides sufficient energy rapidly to activate the main reaction. Usually, a high-quality fuel should react nonviolently and produce nontoxic gases. It should also work as a chelating material for metal cations. During the reaction, metal nitrates perform dual roles of cation source and oxidant. This synthesis process is, in fact, self-sustainable after the reaction has initiated and holds high-temperatures, fast heating rates and short time for reaction. This synthesis method is largely investigated and extensively employed in the large-scale production of the nanosized ZnO powder [Kashinath *et al*. (2002)]. Moreover, combustion method is also reliable and requires low cost raw materials.

2.2. Native Defects in ZnO

ZnO is always accommodated with intrinsic defects which play an important role in conduction, magnetic behaviour and optical properties. Most probable defect types are interstitials, vacancies, antisites, substitutionals, and Frenkel defect pairs. Since they are of crucial importance, we have listed them below and shown in Fig. 2.1:

➢ **Interstitials:** The impurity atom or any lattice atom "A" occupies a position in between the usual lattice sites. Interstitials are denoted by "A_i" (i.e. Zn_i, O_i).

➢ **Vacancies:** A missing lattice atom "A" in the lattice results in a vacancy and deprives the crystal of one electron per broken bond. Vacancies are denoted by "V_A" (i.e. V_{Zn}, V_O).

➢ **Antisites:** A lattice atom "A" of one type occupies the lattice site of another lattice atom "B". Antisites are denoted by "A_B" (i.e. Zn_O, O_{Zn}).

➢ **Frenkel Defect Pair:** The lattice atom "A" is displaced from a lattice site to a nearby interstitial site forming a complex. The defect pair is denoted by "$V_A - I_A$" (i.e. $V_{Zn} - I_{Zn}$).

➢ **Schottky Defect Pair:** The defect forms when oppositely charged lattice atoms "A" and "B" leave their lattice sites, creating vacancies. These vacancies are formed in stoichiometric units, to maintain an overall neutral charge in the ionic solid. The defect pair is denoted by "$V_A - V_B$" (i.e. $V_{Zn} - V_O$).

➢ **Substitutionals:** One of the constituent lattice atoms "A" is replaced by an impurity atom "C". If the impurity atom provides less electrons than the atom it replaces, it will form an acceptor, otherwise a donor. Substitutionals are denoted by "C_A" (i.e. H_{Zn}).

In ZnO, defects could be zinc interstitials (Zn_i), oxygen interstitials (O_i), zinc vacancies (V_{Zn}), oxygen vacancies (V_O, V_O^+, V_O^{2+}) or their complexes [Kohan *et al.* (2000)]. These defects create electronic states in the band gap of ZnO, which influence its optical and electronic properties [Ahn *et al.* (2009)]. In literature, some important issues like green light emission, n-type conductivity, magnetic ordering related to the native defects in pure ZnO have been discussed.
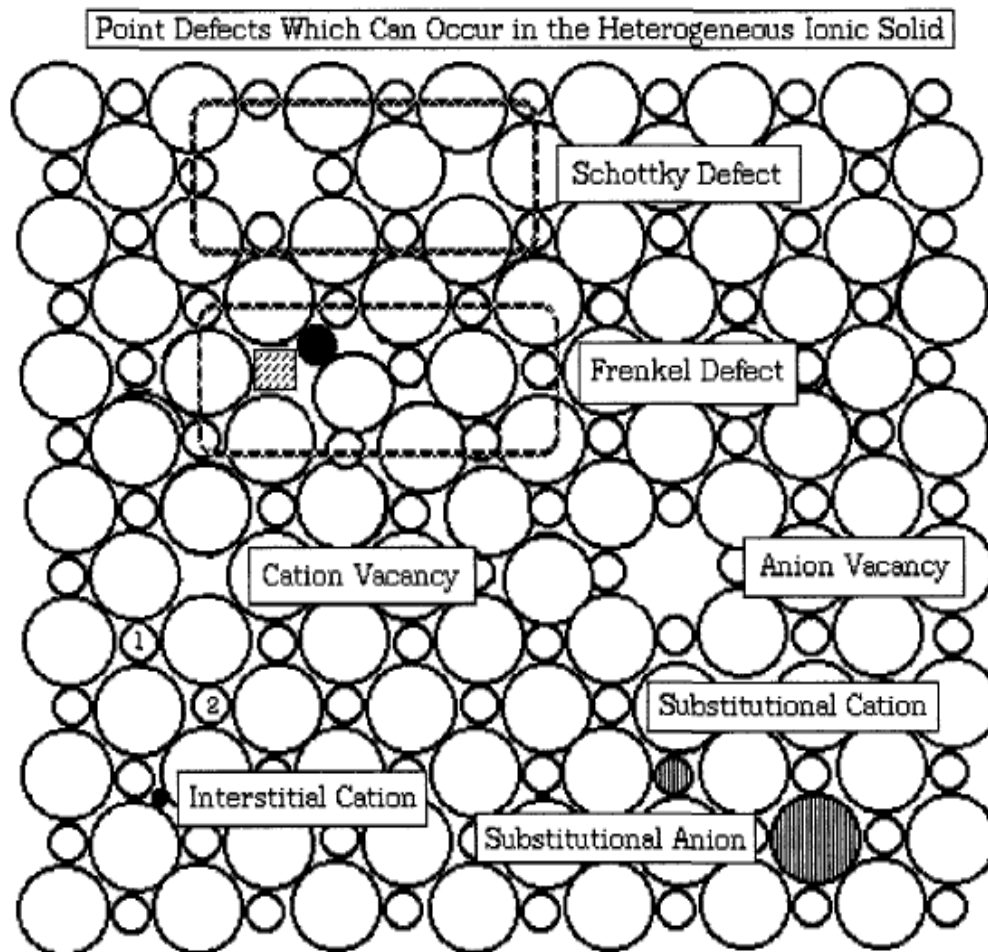
Figure 2.1: Point defects in the heterogeneous ionic solid [after Boon Kuan Woo (2010)].

2.2.1 Green Light Emission in ZnO

ZnO is a well-known greenish white light emitting phosphor for low-voltage vacuum display devices with a relatively high luminescent efficiency [Vanheusden *et al*. (1997)]. ZnO, due to its bio-compatibility, can be used as a suitable phosphor material (by doping) in biological labeling applications [Singh *et al*. (2007)]. Furthermore, doping of ZnO with transition metals leads to efficient phosphors by tuning its green emission into other visible emissions [Zhao *et al*. (2005)]. The green emission of ZnO is applicable in phosphors, on the other hand, this emission degrades the efficiency of ZnO based UV lasers and other UV-devices. Ke *et al*. (2010) have reported the correlation between UV emission and the green emission of ZnO. According to them, when samples are annealed in the presence of oxygen, UV emission improves on

contrary to green emission [Ke *et al.* (2010)]. Now, it is quite commonly accepted that the green luminescence in ZnO arising from a radiative recombination involving an intrinsic defect center is known as defect band emission (DBE). However, the exact mechanism and defect center responsible for this process is still under investigation. In addition to green emission, few other emissions of ZnO like green-yellow (560 nm), yellow-orange (600 nm) and red (650 nm) are also reported [Ahn *et al.* (2009)]. Different defects are found responsible for these different emissions. Özgür *et al.* (2005) have suggested that the DBE may consist of PL bands at similar positions of different origins. Ahn *et al.* (2009) have been proposed an emission band diagram shown in Fig 2.2. Thus, it remains a challenge to correlate the commonly observed 1.9-2.1 eV "red", 2.3-2.5 eV "green" and other luminescence emissions with specific native defects. The emissions vary widely in ZnO bulk and thin films grown by various methods [Ahn *et al.* (2009)]. Ke *et al.* (2010) have found the optical transition in green (535 nm), green-yellow (560 nm) and yellow-orange (600 nm) emission zones. Their studies have demonstrated that the green emission produced in ZnO can be attributed to Zn vacancies while the green-yellow emission is likely to be
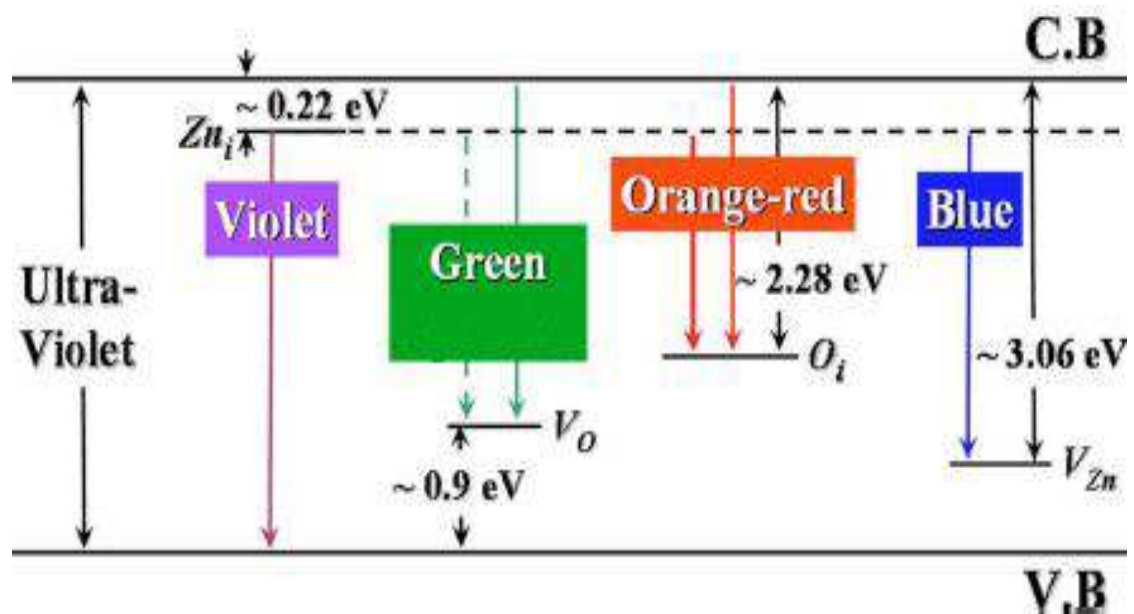

Figure 2.2: Schematic band diagram of near band edge (NBE) and defect band emission (DBE) in ZnO [after Ahn *et al.* (2009)].

due to O vacancies. It is also known that the yellow-orange emission may be caused by O interstitials. S. Y. Myong and K.S. Lim (2007) have speculated that the V_O may be a deep level donor and thus, the green emission at ~2.2 eV can be explained as the transition between V_O and V_{Zn} donor–acceptor pairs [Myong S.Y. and Lim K.S. (2007)]. It is generally assumed that the crystal quality of ZnO is strongly related to the stability of the NBE emission and the intensity ratio of NBE to DBE emission. Ohashi *et al*. (2003) have observed broad visible emission band which is suppressed and, simultaneously, the UV emission intensity at 3.3 eV is increased by more than ten times after H plasma irradiation [Ohashi *et al.* (2003)]. The improvement in UV emission efficiency is ascribed to the passivation of active centers, which are the origin of the visible emission. According to Ohashi *et al.* (2003) speculation regarding the passivation of zinc vacancies is one of the most effective way of improving the UV emission efficiency in ZnO. A similar phenomenon with ZnO nanorods is also reported by Lin *et al.* (2005). It has been shown that the native defects or impurities contributing to visible transition are passivated by H_2 plasma treatment and the PL spectrum of the postannealed ZnO nanorods is almost restored to that of original ZnO nanorods (ZnO nanorods without H_2 plasma treated). The peak shift of 0.2–0.3 eV towards higher binding energies in Zn $2p$ spectrum is observed for H_2 plasma treated ZnO nanorods. However O 1s peak (centered at 531.25 eV), associated with O^{2-} ions in oxygen deficient regions within the matrix of ZnO, does not obviously change with hydrogen plasma treatment. This indicates that the oxygen vacancies cannot be reduced by H_2 plasma treatment to improve the UV emission in ZnO nanorods [Lin *et al.* (2005)]. Zhao *et al.* (2005) have located the visible emission peak at 520 nm, and they referred this emission band as the white light emission band (WLEB), since the color of this emission band is close to white. Zhao *et al.* (2005) have observed that the WLEB is significantly suppressed after Zn implantation. In contrast, the O implantation has much less effect on the WLEB. They argued that V_O or V_{Zn} are the only two possible defects that are involved in the WLEB. After implantations during the annealing, additional Zn atoms in the samples

suppress the creation of the defects that are involved in the WLEB more effectively than additional O atoms. This is consistent if V_{Zn} is involved in the WLEB.

2.2.2 n-Type Conduction in ZnO

The n-type and p-type conduction have been achieved in various semiconductors, like Si [Kim *et al.* (2009)], GaN [Youn *et al.* (2006)], Ge, In_2O_3 and InP [Wang *et al.* (2004); Pan *et al.* (2001); Duan *et al.* (2001); Huang *et al.* (2001)] via various approaches, such as in situ doping during growth, post-annealing, and ion implantation. Although ZnO, II-VI semiconductor, always shows n-type conduction because of native defects, p-type doping of ZnO nanostructures has been difficult and rarely achieved. ZnO suffers from the doping asymmetry problem, as a result of this, *n*-type can be doped rather easily, but *p*-type doping seems to be very difficult. Normally, the doping asymmetry problem appears either due to a low valence-band maximum or a high conduction-band minimum [Zhang *et al.* (1998, 1999)]. For example, ZnTe, CdTe, and diamond are few wide-gap semiconductors in which the valence band lies relatively close to the vacuum level resulting the p-type conductivity. On the other hand, semiconductors like ZnO, ZnSe, ZnS, and CdS possess their valence band relatively far from the vacuum level and therefore, demonstrste *n*-type conductivity [Avrutin *et al.*, (2009)]. ZnO shows *n*-type conductivity with a carrier concentration changing from about 10^{14} to 10^{16} cm^{-3}, with room-temperature mobility $\mu_n \approx 200$ cm^2/Vs [D.C. Look (2007)]. The reason of this n-type conductivity and mobility is reported due to native defects which work as a donor. Moreover, these donor states create serious hindrance in *p*-type doping and known as major "killers" of p-type conduction in ZnO. Significant progress have been made in synthesising p-type ZnO in recent years, but could not be succeeded in controlling the native defects introduced during or after the growth of the material which hinder the development of efficient ZnO based light-emitting devices. Look *et al.* (1999) have attributed *n*-type conductivity to the native defects, Kasai *et al.* (1963) have predicted the native defects to be zinc interstitial (Zn_i) or oxygen vacancy

(V_O) which act like donors in ZnO. However, V_O is a deep donor and Zn_i is reported to have high formation energy in ZnO. First principle calculations have revealed that none of the above native defects exhibit characteristic of a high-concentration of shallow donor [Kohan *et al*. (2000)]. Therefore, it is not responsible for n-type conductivity. C. G. Van de Walle (2000) further suggests that n-type conductivity could be due to the presence of hydrogen atom which acts like a shallow donor when present in the interstitial site of ZnO lattice. The ionization energy of a hydrogen donor is found~ 35 – 40 meV [Cox *et al*. (2001); Hofmann *et al*. (2002)]. The behaviour of hydrogen atom in ZnO is, however, unexpected as hydrogen in most of the semiconductors acts like a compensating centre counteracting the existing conductivity. The non amphoteric nature of H in ZnO has also been observed in other II–VI semiconductors. In ZnO bulk or nanostructures, the source of this hydrogen is the water used as solvent in co-precipitation method or hydrothermal method during synthesis. The ZnO surface is able to split the water and generate hydrogen [Ma *et al*. (2010)]. Moreover, hydrogen in thin films synthesised through metal-organic chemical vapour deposition (MOCVD) technique is due to diffusion at elevated temperature of, *e.g.,* 600 °C, where MOCVD technique utilises hydrogen to create reducing environment during thin film deposition [Look *et al*. (2003); IP *et al*. (2003)]. At the same time, the source of the hydrogen could be hydroxyl ions (OH^-) that sometimes serve as passivator for acceptors [Čížek *et al*. (2008)].

2.2.3 Ferromagnetism in ZnO

ZnO is a diamagnetic material. However, ferromagnetism has been observed in ZnO nanostructure experimentally. The observation of ferromagnetism in undoped ZnO has been opened up a wide debate on its origin. The native defects such as O and Zn vacancies are reported to be responsible for the observed ferromagnetism [Liu *et al*. (2005)]. Instead of ZnO, few other undoped metal oxides such as TiO_2, CeO_2, Al_2O_3, In_2O_3, and SnO_2 are also reported for demonstrating room-temperature ferromagnetism [Sundaresan *et al*. (2006)]. Sundaresan *et al*. (2006) have predicted that the

origin of ferromagnetism in undoped metal oxide could be due to the exchange between unpaired electron spins arising from oxygen vacancies at the surfaces of the nanoparticles. Banerjee *et al.* (2007) have observed the enhancement of ferromagnetic contribution in pure ZnO sample upon thermal annealing. They have attributed the enhancement of ferromagnetism to the formation of oxygen vacancy clusters upon thermal annealing. On the other hand experimental results of Wang *et al.* (2010) have supported V_{Zn} behind ferromagnetism. Theoretically, Zuo *et al.* (2009) have calculated the magnetic moment with respect to the various defects present in ZnO and predicted that both I_O and V_{Zn} may induce ferromagnetism in ZnO with the magnetic moment 2.0 μ_B and 1.77 μ_B, respectively. The magnitude of induced magnetic moment in oxygen atom around vacancy site is reported in the range of 0.5 to 0.7 μB [Wang *et al.* (2008)]. Using first-principles calculation, Wang *et al.* (2008) have examined the electronic properties and magnetism of ZnO thin films and nanowires by taking care of both Zn and O vacancies. According to Wang *et al.* (2008), Zn vacancies introduce spin polarization at the top of the valence band and have observed magnetism in ZnO thin films arising indeed from Zn vacancies. These vacancies prefer to reside on the surface, as has been suggested from experiments. The origin of magnetism does not result from the Zn $3d$ electrons but from the unpaired $2p$ electrons of O atoms in the immediate vicinity of the Zn vacancies. Compared to thin films, it is not only easier to introduce Zn vacancy in ZnO nanowire, but the resulting magnetic moment is also larger. Wang *et al.* (2008) have proposed some applications such as magnetic healing, oxygen delivery, improving biofluid circulation for effective transport and release, helping to bring a normal charge back to each body cell via increasing cellular oxygen, and restoring pH balances by using low dimensional magnetic ZnO nanostructure where the magnetism is induced by introducing Zn vacancies instead of doping with transition-metal atoms. Magnetism in pure ZnO provides some advantages as the absence of transition-metal atoms may prevent the formation of dangerous free radicals. According to Kim *et al.* (2009), the ferromagnetism in ZnO cannot be obtained simply by oxygen or

zinc vacancy defect itself, instead, it is realized that the lattice distortion plays an essential role for the vacancy induced ferromagnetism. Interestingly, Kim *et al*. (2009) have explored the Zn vacancy defect inducing ferromagnetic state in ZnO with magnetic moment ranging from 0.1 μ_B to 0.19 μ_B. They have mentioned that the lattice distortion due to Zn vacancy defect plays an essential role for the ferromagnetism in ZnO. Without lattice distortion, the ferromagnetism becomes unstable. Instead of the native defects as reported above, a new source of ferromagnetism in ZnO has been tntroduced, known as hydrogen impurity. In hydrogenated ZnO film, Li *et al*. (2011) have found that OH attached to ZnO surface is responsible for ferromagnetism. Theoretically the magnetic moment is 0.30 μ_B per OH [Li *et al*. (2011)]. They have concluded from the XPS study that H in ZnO strongly bind with oxygen atom, forming an O-H bond and demonstrate that FM ordering could be switched between on and off states by introducing (via hydrogenation) and removing (via subsequent annealing in Ar) OH ion to ZnO surface, respectively. Despite all these efforts, the exact mechanism of ferromagnetism due to native defects or hydrogen impurity in ZnO is not clearly understood because both, experimental and theoretical investigations on the defect or impurity induced ferromagnetism of ZnO, are still in early stage. Therefore, it is of prime importance to detect the defects through various advanced techniques.

2.3 Doping and/or Codoping in ZnO

ZnO have been doped with various metal and non-metal ions for exploring its applicability in the field of optoelectronics and spintronics [Pan *et al*. (2008); Liu *et al*. (2005); Ohtomo *et al*. (1998); Vigil *et al*. (2000); A. Janotti and C. G. Van de Walle (2009)]. Incorporating transition metal ions (TM) in ZnO is found to be less difficult than incorporating them in other semiconductor hosts, since the valence of Zn (2+) can be readily adopted by many 3d transition metal ions. Including different transition metal ions such as Ni, Co, Fe, Mn and Cr many other dopant ion like Mg, Cd, Li, Na, K, Ag, Al, N, P etc. are reported for successful doping in ZnO. The main aim behind the doping in ZnO is to substitute the dopant at the cationic or anionic site with

higher concentrations and enhance the electrical, optical and magnetic behaviour with respect to doping. Table 2.1 lists the valence and ionic radii of different dopants in ZnO.

Table 2.1 Valence and ionic radii of possible candidate of dopant atoms

Atom	Valence	Radius (A°)
Li	+1	0.59
Na	+1	1.02
K	+1	1.51
Ag	+1	1.00
Mg	+2	0.72
Mn	+2	0.67
Fe	+2	0.61
Co	+2	0.65
Ni	+2	0.44
Cu	+2	0.57
Zn	**+2**	**0.60**
Cd	+2	0.78
Cr	+3	0.62
Al	+3	0.39
Ga	+3	0.47
In	+3	0.62
N	-3	1.46
P	-3	2.12
As	-3	2.22
Sb	-3	2.45
O	**-2**	**1.36**
F	-1	1.33

2.3.1 Optical Properties of Doped/Codoped ZnO

ZnO has large band-gap of ~3.4 eV and emits light in ultraviolet region. Modern ZnO based optoelectronic devices require the understanding of band-gap engineering to generate UV laser. The band gap engineering (tailoring) at the ultraviolet and visible region of the solar spectrum is of considerable interest for large area of optical coatings. Already, GaN and its alloys have been recommended for the application of blue lasers. The visible portion of the spectrum can be covered by semiconductor diodes. However, there are still major improvements to be made in these devices at the UV-region. Band-gap engineering in ZnO can be achieved by doping (alloying) with Mg (MgO) and/or Cd (CdO), in correlation to GaN which can be doped (alloyed) with Al (AlN) and/or In (InN) [Anderson Janotti and Chris G Van de Walle (2009)]. As an alternative to the GaN material, doped ZnO appears to have great potentiality for ultraviolet light emitters, and truly solar blind photodetectors, which are transparent to the visible and near-UV portion of the spectrum. Moreover, this also suggests the possibility of hybrid optoelectronic devices comprised of lattice-matched MgZnO/AlGaN heterojunctions [Osinsky *et al.* (2004)]. Doping (alloying) ZnO with Mg (MgO) or Cd (CdO) allows the band gap to be controlled between 2.8 and 4 eV and higher, which facilitates band gap engineering. However, MgO and CdO possess the rock-salt structure, unlike ZnO (wurtzite structure) due to which the possibility of doping (solubility limit) of Mg (MgO) or Cd (CdO) is restricted in ZnO [Roessler *et al.* (1967)]. According to the phase diagram of the ZnO-MgO binary system, the thermodynamic solid solubility of MgO in ZnO is less than 4 mol % [Segnit *et al.* (1965)]. This is indeed a problem for doping (alloying) ZnO with high content of Mg (MgO) or Cd (CdO), in which the phase separation is expected to occur. On the other side, Ohtomo *et al.* (1998) have reported the synthesis of Mg doped ZnO with a Mg content of upto 33%. Above 33% of Mg content in ZnO, a secondary phase of MgO segregates in addition to the wurtzite ZnO. By Mg doping, Ohtomo *et al.* (1998) have observed an increase in band gap upto 3.9 eV without segregation of any impure phases. In comparison to ZnO an

increase in the exciton binding energy has been observed for Mg doped ZnO [Ohtomo *et al*. (1998)]. Although MgO has rock-salt structure, the ion radii of Mg^{2+} (0.57A°) and Zn^{2+} (0.60A°) are so similar that Mg^{2+} can replace the location of Zn^{2+} in ZnO with fairly small lattice mismatch (0.1%). Therefore, with increasing Mg content in ZnO, it still possesses the wurtzite hexagonal structure, and the cell volume hardly changes even for high Mg concentration. The increase in band gap of ZnO with Mg doping is due to the wide band gap of MgO which is 7.7 eV [Shan *et al*. (2004)]. Further, the thermal stability of wurtzite-phase in Mg doped ZnO samples have been studied by Ohmoto *et al.* (1998) Upto 15% of Mg doping, ZnO is found to be stable with elevated annealing temperature above at 850 °C. Above 15% of Mg doping in ZnO, segregation of MgO is started at 850 °C. The band gap is also reduced to the value equal to the band gap of 15% Mg doped ZnO after annealing at 1000 °C [Ohtomo *et al*. (1998)]. A decrease in the band gap down to 2.99 eV has been achieved by doping Cd upto 7% in ZnO [Makino *et al*. (2001)]. This decrease in band gap of ZnO with Cd doping is due to the small direct band gap of CdO which is 2.3 eV. In the case of Cd doping in ZnO, the lattice volume increases with the Cd content. This increase in lattice volume is due to the larger ion radii of Cd^{2+} (0.78 A°) as compared to Zn^{2+} (0.60A°). Cd^{2+} replaces the Zn^{2+} in ZnO with the lattice mismatch of 0.5% with respect to ZnO [Makino *et al*. (2001)]. On the other hand, in Cd-doped ZnO quantum dots (QDs), a blue shift has been observed with the increasing concentration of Cd. This shift is due to the quantum confinement effect. The diameters of these samples are found to decrease from 6, 5.2, 3.6, 3.3 and 3.2 nm for 0.0, 0.02, 0.05, 0.10 and 0.20 at% doping of Cd in ZnO, respectively [Zhang *et al*. (2012)]. In addition to Mg and Cd, few reports demonstrate the doping of ZnO with other transition metals such as Cr, Mn, Fe, Co, Ni, Li and Al which offers a viable means of tuning the band gap [Joseph *et al*. (2011); Rakkesh *et al*. (2014); Rahman *et al*. (2012)]. By using diffuse reflectance spectrocopy (DRS), which is particularly appropriate for the determination of absorption edges of powdered materials, Joseph *et al*. (2011) have calculated the band gap for $Zn_{0.95}TM_{0.05}O$ (TM = Cr,

Mn, Fe, Co, & Ni) samples. The band gap variation for $Zn_{0.95}TM_{0.05}O$ (TM = Cr, Mn, Fe, Co, & Ni) samples are shown in Fig. 2.3. The band gap calculation by Rakkesh et al. (2014) comes out to be 3.19, 3.23, 3.24 eV for 0.0, 0.05 and 0.10 at% of Li doping in ZnO, respectively. Rahman et al. (2012) have shown the band gaps variation for Al-doped ZnO for different concentration of Al (0.0, 0.01, 0.02, 0.03 and 0.04 at%). It is found that the estimated band gap energies decrease from 3.28 eV to 3.05 eV with increasing doping of Al from 0 at% to 4 at%.

Moreover, by doping with luminescent centers such as transition or rare-earth metal ions, the emission properties of ZnO can be tailored toward selected wavelengths in the visible region, which is of interest for a variety of applications including multicolor emission in light emitting devices [Panatarani et al. (2004); Lima et al. (2002)]. In several reports, PL spectroscopy is used to study emission properties of doped/codoped ZnO, as well as it can reveal about the relative concentration of defects in the samples. For example, Er^{3+}-doped ZnO systems have been studied extensively for the red emissions [Kohls et al. (1999); Komuro et al. (2000)]. Tb^{3+}-doped ZnO has been studied a great deal as a green luminescence material [Yan et al. (2007); Monteiro et al. (2006)]. The effect of annealing atmosphere, temperature and aging on the photoluminescence of pure and Li-doped ZnO have been investigated by Wang et al. (2011). The visible emission of the Li-doped ZnO is found to be largely dependent on the annealing atmosphere. Moreover, from PL study, the substitutional and interstitial extrinsic point defects created by lithium doping may mediate the relative concentration of the intrinsic defects and thereby, tune the intrinsic-defect-related visible emission [Wang et al. (2011)]. Yellow luminescence in ZnO containing no foreign impurities can be considered to be intrinsic due to an excess of oxygen. On the other hand, on doping Mn in ZnO, the luminescence band of pure ZnO is redistributed and the luminescence colour changes from yellow to dark red in accordance to the Mn concentration in ZnO [Liu et al. (1992)]. Incorporation of dopants like Fe, Co, and Mg at host lattice sites enhance the defect emission compared to band edge emission

observed in PL spectra [Inamdar *et al*. (2011); Cui *et al*. (2006); Peng *et al*. (2006)]. The Cu related defects are considered to be an important reason that causes green emission besides intrinsic defects such as oxygen vacancies [Wan *et al*. (2013)]. The PL intensity of defect related peak at 518 nm increases due to the incorporation of Cu and/or Co in ZnO, but the UV emission peak diminishes in correlation [Wan *et al*. (2013)]. The emission spectra of Cd doped ZnO show the increase in the intensity of UV as well as visible emission significantly with increasing Cd concentrations (Zhang *et al*., 2012).
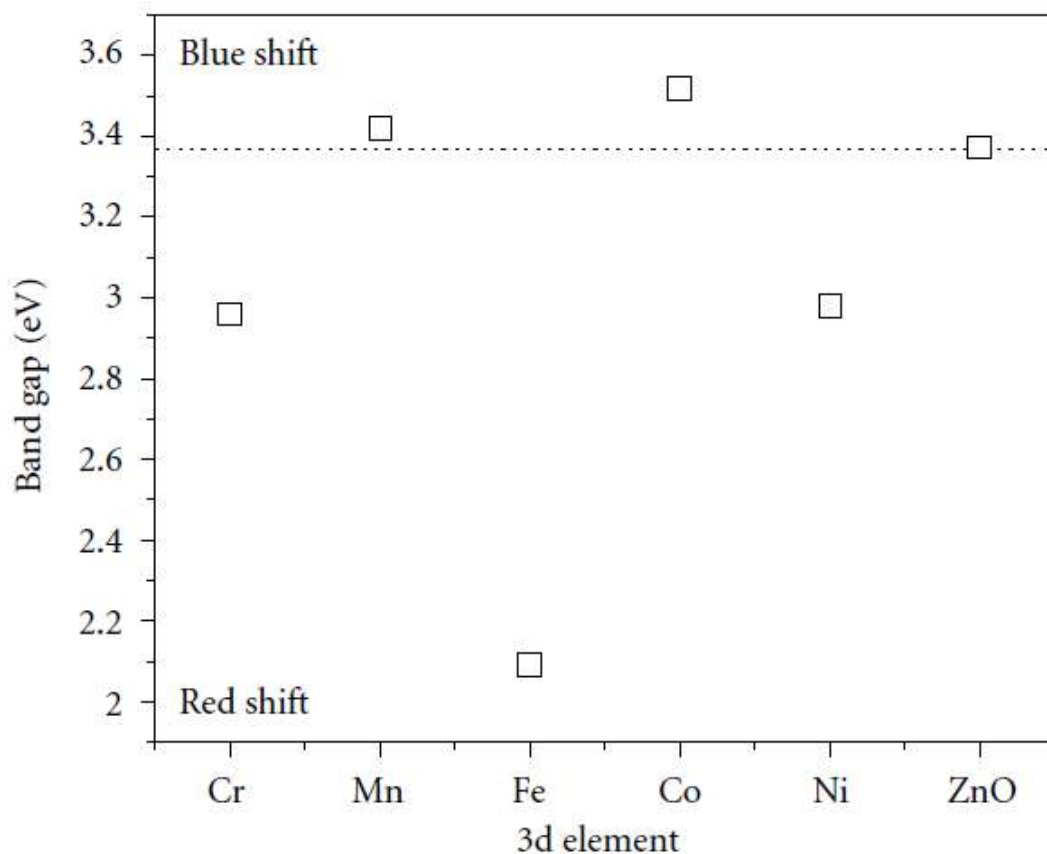

Figure 2.3: Variation in band gap of transition metal (TM= Cr, Mn, Fe, Co, & Ni) doped ZnO for $Zn_{0.95}TM_{0.05}O$ composition (after D. Paul Joseph and Venkateswaran, 2011).

2.3.2 Magnetic Properties of Doped/Codoped ZnO

The field of spintronics exploits both electron spin and its charge in order to introduce an additional degree of freedom to the next generation of electronic devices. Generally, the substitution of cations by magnetic transition metal ions such as Fe, Co, Mn, Ni in III-V or II-VI nonmagnetic

semiconductors allows the charge and spin degree of freedom in a single substance which leads to a number of magnetic, optical and magneto-optical phenomena. For example, doping ZnO with transition metal ions like Mn, Fe, or Co, known as dilute magnetic semiconductors, show FM order due to injection of magnetic spin into the matrix [Ueda *et al.* (2001)]. The most common DMSs are III-V and II-VI compounds (CdTe, ZnSe, CdSe, ZnO, GaN, GaAs), doped with transition metal ions which may be used as spintronics materials [Photongcam *et al.* (2010)]. But for room temperature application of spintronic material, ZnO and GaN materials have been predicted theoretically to be the most promising material as compared to the other II-VI (such as CdTe, ZnSe, CdSe, CdS, etc.) and III-V (GaN, GaAs, AlN, etc.) compounds [Liu *et al.* (2005)]. While few papers show ZnO:Co [Venkatesan *et al.* (2004)], ZnO:Ni [Jin *et al.* (2001)], and ZnO:Mn [Jin *et al.* (2001)] are paramagnetic in nature, the others have reported ferromagnetism in Co and Mn doped ZnO [Venkatesan *et al.* (2004)], both in bulk as well as in thin film form. Several studies have found that ferromagnetism depends strongly on methods and the conditions of preparation [Sluiter *et al.* (2005)]. Moreover, in some reports, defects are found to play a crucial role in showing FM in TM-doped ZnO [Coey *et al.* (2005)]. For example, defects like V_O and/or Zn_i lead to RTFM and are even found responsible for enhancement in magnetic moment [Liu *et al.* (2007); Song *et al.* (2006); MacManus-Driscoll *et al.* (2007); Hsu *et al.* (2007), Liu *et al.* (2007)]. Few reports have shown that annealing the samples in a reducing atmosphere (such as vacuum [Chakraborti *et al.* (2007); Ramachandran *et al.* (2006); Liu *et al.* (2007)] and Ar/H_2 [Hsu *et al.* (2006)]) create V_O which greatly enhance RTFM in TM-doped ZnO. The enhanced FM due to the formation of V_O is also reported in TM-doped ZnO films deposited in vacuum [Song *et al.* (2006); Li *et al.* (2008); Krishnamurthy *et al.* (2006)]. The enhancement in FM due to Zn_i defect is found in Co-doped ZnO films as well as in nanocrystals, which are annealed in a Zn atmosphere [MacManus-Driscoll *et al.* (2007); Schwartz *et al.* (2004)]. In some TM-doped ZnO films and nanowires, the edge dislocations accompanied with V_O and/or Zn_i point

defects, which have confirmed by HRTEM, increase the RTFM [Zhang *et al*. (2006); Herng *et al*. (2006); Song *et al*. (2007); Jian *et al*. (2006)]. Wan et al. (2013) have found that the coexistence of donor defects (Zn_i and V_O) and Cu ions are responsible for the obvious room temperature ferromagnetism (RTFM) in Cu doped ZnO and the RTFM is attributed to an indirect double-exchange interaction associated with dual donor defects. The origin of ferromagnetism and exact nature of the ferromagnetic coupling of spins in ZnO is a matter of debate till date.

A number of new experimental and theoretical approaches have been developed to achieve RTFM and describe the mechanism of DMS related with transition metal doped ZnO systems; very often such theories contradict each other in their basic assumptions and final conclusions. Because Co ion possesses high magnetic moment (1.9 μ_B per Co) at RT among all other transition metal ions in (Zn,TM)O [Venkatesan *et al*. (2004)], therefore ZnO:Co is widely studied DMS material in this context. The solubility of Co ion in ZnO upto 15 % is reported [Jin *et al*. (2001); Fukumura *et al*. (1999)]. However, for polycrystalline sample of Co doped ZnO system studied by Lee *et al*. (2005) has shown that samples retain single phase only upto 5 % dopant. According to Lee *et al*. (2010), as dopant concentration is raised to 10 % a Co_3O_4 impurity phase appear, which increases with the dopant concentration. Similarly, some other literatures already have reported Co_3O_4 impurity phase during the study of Co doped ZnO. It is extremely difficult to detect secondary phases such as Co_3O_4, CoO and Co nanoclusters even with high resolution x-ray diffractometer [Ney *et al*. (2010)]. Rath *et al*. (2009) have synthesised $Zn_{1-x}Co_xO$ and have shown single phase upto 20% of Co. They have demonstrated peak broadening in XRD at and above 5% of Co doping in ZnO, which is due to an anomalous strain rather than particle size. The strain is developed due to antiferromagnetic interaction of Co which leads to paramagnetism at RT. By controlling the donor defects like zinc interstitial (Zn_i), Shah *et al*. (2009) have demonstrated the switching between ferromagnetism and paramagnetism in Co doped ZnO system. These

controversial results raise questions about the origin and the intrinsic nature of ferromagnetism in Co-doped ZnO.

Further, a computational study by Spaldin *et al.* (2004) has shown that the ferromagnetic ground state is not favoured in Co doped ZnO without additional carrier doping and have suggested that codoping with Cu is an alternating route for increasing the carriers in Co doped ZnO for realizing room temperature ferromagnetism. Lathiotakis *et al.* (2008) have demonstrated that an optimum structural dopant configurations which lead to enhancement of ferromagnetism in (Co,Cu) codoped ZnO. The role of the Cu^+ ion is to act as super exchange mediators by causing a remote delocalisation through the hybridisation of the Cu $d_{3z^2-r^2}$ spin-majority states with the O p states, thereby enhancing the ferromagnetism [Lathiotakis *et al.* (2008)]. Similarly, some experimental data claiming that FM can be switched in Co doped ZnO by adding Cu, Al and Li which increases the carrier concentration [Liu *et al.* (2006)]. Jayakumar *et al.* (2005) synthesised (Co, Cu) codoped ZnO by co-precipitation method in organic medium and observed ferromagnetic behaviour for $Zn_{.94}Co_{.05}Cu_{.01}O$ annealed at 725 K and paramagnetic behaviour for $Zn_{.95}Co_{.05}O$ at RT. Sluiter *et al.* (2005) have argued theoretically that Co has the best potential for Zn substitution in ZnO when combined with a hole dopant like Li or an electron dopant like Cu. As per their theoretical prediction, room temperature ferromagnetism in ZnO:Co may be enhanced after codoping Li [Sluiter *et al.* (2005)]. Liu *et al.* (2006) have reported that codoping Al in Co doped ZnO also induces carrier mediated ferromagnetism. On the other hand, no FM is found in structurally excellent Al-codoped ZnO [Ney *et al.* (2010)]. Similarly, Alaria *et al.* (2006) have reported that Al doped $Zn_{.9}Co_{.1}O$ show no ferromagnetism in spite of the creation of free carriers. Behan *et al.* (2008) have shown that there are two distinct mechanisms for ferromagnetism in doped ZnO such as by varying carrier densities (e.g., produced by Al) and magnetic polarons and carrier-mediated exchange. At low carrier densities, magnetic polarons give rise to FM. At high carrier densities, the magnetisation

depends on the carrier density, as predicted by the theory of carrier-mediated exchange [Bhen *et al*. (2008)].

Therefore, several dopants like Co, Ni, Mn, Fe, Sb, Cu, Li, Mg, Al and Ga and codopants like Al and Co, Mn and Co and Ga and Co etc. are incorporated in ZnO matrix to study their structural, optical, electrical and magnetic properties [Bhen *et al*. (2008), Yan *et al*. (2004), He *et al*. (2008)]. Overall, defects whether it present in ZnO or appeared after doping/codoping play a significant role in controlling above properties and produce major hindrances to fabricate the devices. Therefore, the key issue for achieving the above properties with optimum value is the detection and prevention of defects and/or impurities in doped/codoped ZnO during growth.

2.4 Ceramic Composites

Ceramic composites are of great interest for photonic devices. The most common approach for the development and easy manipulation of such composites with enhanced luminescent and/or photocatalytic properties are to combine a filler with particular optical and/or catalytic property with a ceramic host matrix. Transition metal oxides like ZnO [Djurisic *et al*. (2004)], TiO_2 [Bahadur *et al*. (2010)], MgO [Das *et al*. (2005)], and SnO_2 [Gu *et al*. (2013)] etc. have been considered as the most common fillers for the next-generation light-emitting devices and photocatalyst. For example, composites formed of TiO_2 modified MoO_3 show an interesting red shift in their photoresponse [Elder *et al*. (2000)]. The photoabsorption energy required to promote TiO_2 valence band electrons to MoO_3 conduction band states systematically shifted from 2.88 to 2.60 eV by tuning the size in between 4 and 8 nm [Elder *et al*. (2000)]. TiO_2 shows enhanced luminescence intensity. Persistent luminescent for 3 h after turning off the light source for photocatalytic reaction has been observed in $CaAl_2O_4/TiO_{2-x}N_y$: (Eu, Nd) composite [Li *et al*. (2010, 2012, 2012(b))]. $SrAl_2O_4$ with TiO_2 has been used in solar cell as it has an improved efficiency and light down-converting properties of phosphors in presence of Eu, Dy rare earths [Sun *et al*. (2013)]. Dye-sensitized photovoltaic cells based on TiO_2 and TiO_2 based composites have been extensively studied in recent years [Bach *et*

al. (1998)]. However, due to upward shift of conduction band edge, cells made from SnO_2 and ZnO composite (instead of TiO_2) have shown higher photocurrents [Tennekone *et al*. (1999)].

2.4.1 ZnO Based Ceramic Composites

ZnO based composites have its own importance due to the green emission of ZnO which is applicable for greenish white light emitting phosphor for low-voltage vacuum flat panel display devices with a relatively high luminescent efficiency [Djurisic *et al*. (2004); Bylander *et al*. (1978)]. Moreover, ZnO improves the UV shielding in different host as encapsulating material [Li *et al*. (2006)]. However, in order to reduce the power consumption and increase the luminescence efficiency in ZnO-based nanocomposites for the above application, a basic physical understanding of the luminescent processes of the composite materials is essential. The use of ZnO-based nanocomposites are also proposed in ceramic technology for application in varistors, sensor elements, photoconductors in electrophotography [Cannas *et al*. (1999)], and electroluminescent applications such as in photoelectronics integrated devices, and semiconductor lasers. In a broad perspective, practical use of ZnO based composites, exploring the various defects present in ZnO, their role on different properties of composites, as well as methods of their production is of current challenge. While formation of ZnO based ceramic composite shows improvement in catalytic behaviour [Lin *et al*. (2006)], optical properties show enhancement in photon emission. Several host materials like ZnS [Gao *et al*. (2013)], CdS [Ling *et al*. (2011)], CdSe [Lu *et al*. (2012)], PbS [Vogel *et al*. (1994)] SiO_2 [Chen *et al*. (2004)], YbF_3 [Zhang *et al*. (2013)], Y_2O_3 [Yadav *et al*. (2013)], $ZnGa_2O_4$ [Zhong *et al*. (2012)], $ZnAl_2O_4$ [Hou *et al*. (2010)] and $CaAl_2O_4$ [Verma *et al*. (2011)] have been assembled with ZnO filler. For example, ZnO-ZnS composite shows improvement in the performance of dye-sensitised solar cells [Chung *et al*. (2010)]. Coupling ZnO with CdS or CdSe, the incident photon to current conversion efficiency (IPCE %) is enhanced significantly in ZnO-CdS or ZnO-CdSe composites, respectively [Hotchandani *et al*. (1992)]. In ZnO-CdS or ZnO-CdSe composites, CdS or CdSe acts as a

visible sensitiser and ZnO, being a wide band gap (3.34 eV at 2 K) semiconductor, is responsible for charge separation which suppresses the recombination process [Nayak *et al*. (2008)]. Yao *et al*. (2000) have reported band gap luminescence from ZnO in mesoporous silica, and they have found that Zn-O-Si cross-linking bonds that formed at the interface between ZnO and the pore walls of silica which influences the optical properties of ZnO-SiO_2. Much attention has been paid to the UV barrier properties of fabrics modified with ZnO-SiO_2. ZnO nanorods in combination with CuO nanoparticles offer considerable promise for the photocatalytic production of hydrogen from aqueous solution by exposing them to solar radiation [Simon *et al*. (2012)]. The unique and controllable structural and electrical properties, good stability and corrosion resistance of carbon materials offer a fertile playground to fabricate a variety of ZnO-carbon hybrid composite materials for photocatalytic applications [Fan *et al*. (2012), Akhavan *et al*. (2010), Xu *et al*. (2010)]. Normally, due to the inherent low conduction band edge of SnO_2, leading to theoretically low photovoltage and the fast recombination process in SnO_2 reveal the lower performance in SnO_2 based devices [Green *et al*. (2005)]. On the other hand SnO_2/ZnO based dye-sensitized cell show higher long-term stability relative to the TiO_2 counterpart [Tennakone *et al*. (1999)]

2.4.2 ZnO Based Spinel Composite

ZnO also plays a significant role when used in spinal matrices like $ZnGa_2O_4$, $ZnAl_2O_4$, $CaAl_2O_4$ and $SrAl_2O_4$. The spinels generally contain large number of intrinsic defects that basically improve the catalytic and luminescent properties [Zhong *et al*. (2012); Hou *et al*. (2013); Verma *et al*. (2011, 2012); Zhuang *et al*. (2013)]. Spinels show better emission due to the presence of high concentration of cationic vacancies and a large proportion of intrinsic disorder [Gritsyna *et al*. (2002)]. Intrinsic defects in the spinels act as trapping centers for electrons and holes created by irradiation. Hou *et al*. have shown different luminescence bands with different intensities by exciting with He-Cd laser in ZnO and $ZnAl_2O_4$ composite. The intensity of luminescence is found to be 15 times higher in ZnO-$ZnAl_2O_4$ composite than that of ZnO [Hou *et al*. (2013)].

The comparative study of ZnO and ZnO-ZnGa$_2$O$_4$ composite are reported by Zhong *et al*. (2012). Compared to the ZnO nanowire array, a more favourable energy band position for the photo-electrolysis of water and an increased carrier density for the electron transfer are obtained in ZnO-ZnGa$_2$O$_4$. Woo (2010) studied the effect of nano ZnO in the spinels such as CaAl$_2$O$_4$ and SrAl$_2$O$_4$. The persistent luminescence property in ZnO-CaAl$_2$O$_4$ phosphor is diminished. According to Woo (2010), ZnO repairs the internal lattice defects of CaAl$_2$O$_4$ phosphor that causes the reduction of electrons trap density. On the other hand, in ZnO-SrAl$_2$O$_4$ phosphor, it has been proposed that the presence of nano ZnO induce internal lattice defects that act as electrons trap. Hence the combination of both electrons trap and holes trap improves the persistent luminescence property of this phosphor. Besides, SrAl$_2$O$_4$ has been proven to be an efficient host material for photo luminescence, cathodoluminescence and plasma display panel phosphors in visible region [K. D. Budd *et al*. (1995)]. The preparation of pure SrAl$_2$O$_4$ is quite troublesome as without using any flux it requires high temperature.[Escribano *et al*. (2005)] The integration of ZnO with SrAl$_2$O$_4$ rich in intrinsic defects may make them possible to achieve excellent photoluminescence (PL) properties. Due to large lattice mismatch between ZnO and SrAl$_2$O$_4$, new defects generate at the ZnO/SrAl$_2$O$_4$ interface that may further improve the luminescence.

SrAl$_2$O$_4$ displays two polymorphs: monoclinic (MP) and hexagonal (HP). Below 650 ^{o}C, it exhibits monoclinic phase, P2$_1$ and above, it turns into a hexagonal phase, P6$_3$22 [Fukuda *et al*. (2005); Avdeev *et al*. (2007)]. The transformation is an endothermic process with a change in enthalpy ΔH = 3.2 kJ/mol and the reverse transformation is an exothermic one [Douy *et al*. (2003)]. Monoclinic phase, being a stable phase at room temperature, is well known to be stuffed tridymite derivative. However, the preparation of such phase without flux requires very high temperature [Levin *et al*. (1964)]. It is therefore a technological issue to reduce the temperature of synthesis as it is used as a phosphorescent material for visible region. Escribano *et. al.* (2005) synthesised SAO through a modified sol-gel route at much lower temperature

compared to the ceramic route by adding boron to it. On the other hand, hexagonal phase, which is a metastable phase at room temperature, can be stabilised by insertion of a small amount of Ca [Prodjosantoso *et al.* (2002)], Ba [Henderson *et al.* (1982); Wu *et al.* (2009)], B [Jung *et al.* (2006)] or excess Al or by quenching from high temperature [Douy *et al.* (2003); Dong-dong *et al.* (2000)]. By quenching from high temperature, one may end up with an unstable and incomplete transformation from monoclinic to hexagonal phase [Dong-dong *et al.* (2000)]. There is hardly any report where hexagonal phase of SAO has been synthesised at room temperature without any dopant.

Significant progress has been made on producing long persistent visible light emitting phosphors when SAO having two polymorphic phases (monoclinic and hexagonal) doped with rare earth metals [Katsumata *et al.* (2006); Aizawa *et al.* (2003); Katsumata *et al.* (2006); Murayama *et al.* (1995)]. Dong-Dong *et al.* (2000) have shown that hexagonal phase of SAO doped with Eu has higher light emission efficiency than that of the monoclinic one [Dong-dong *et al.*]. Wu *et al.* (2009) have observed blue shifting in the emission spectra with the gradual phase transformation of SAO from monoclinic to hexagonal. However, there are some reports where only the monoclinic phase of SAO shows luminescent properties when doped with rare earth ions [Katsumata *et al.* (2006); Jia *et al.* (1998); Kato *et al.* (1999)]. The higher quantum efficiency of luminescence is observed in monoclinic SAO doped with Eu, Dy than in hexagonal SAO [Shafia *et al.* (2010)]. On the other hand, significant work has been pursued in tailoring the optical properties by making composites of SAO with polymers like PVP (Poly vinyl pyrrolidone) and PMMA (Polymethyl methacrylate) [Zheng *et al.* (2011); Yina *et al.* (2006)]. In view of the above discussion, one may conclude that both hexagonal and monoclinic phase carry equal importance as far as the luminescent properties are concerned. But the real challenge lies in the synthesis of high tempertaure hexagonal phase at RT in order to use them in optoelectronic devices.

2.5 Objectives of the Present Work

Compiling the literatures, one may precisely say that in its own right "defects in ZnO" has become one of the most discussed issues in condensed matter physics and material science at present. A delicate balance of various defects in ZnO gives rise to fundamentally new and newer material characteristics. Thus detection of defects plays an important role in this field of research. One may be able to tune these defects for various applications that ZnO possess.

The objectives of the present study are as follows:

➢ To study the growth of various morphologies of ZnO varying the pH of precipitation under coprecipitation route. To investigate the native defects in ZnO (synthesized by coprecipitation, sol-gel and combustion techniques) through various spectroscopic techniques like XRD, Raman, PL and PAS.

➢ To determine the structural modification, the optical and magnetic properties with respect to defect in Mg doped as well as Mg and Co codoped ZnO samples.

➢ To examine the role of ZnO in modifying the structure as well as the luminescent properties of ZnO-SrAl$_2$O$_4$ composite with varying ZnO concentration.

The results of the present investigations are discussed in the subsequent chapters.